Biochemistry & Analytical Biochemistry

Shima et al., Biochem Anal Biochem 2015, 4:4
DOI: 10.4172/2161-1009.1000213

Research Article Open Access

# Slow Unfolding Pathway of the Hyperthermophilic Tk-RNase H2 Examined by Pulse Proteolysis Using Mutant Proteins

**Kanako Shima, Ai Nagao, Jun Okada, Satoshi Sano and Kazufumi Takano***

*Department of Biomolecular Chemistry, Kyoto Prefectural University, Kyoto, Japan*

## Abstract

The unfolding of ribonuclease H2 from the hyperthermophilic archaeon *Thermococcus kodakarensis* (Tk-RNase H2) is remarkably slow. In previous work, Tk-RNase H2 unfolding intermediates, $I_A$-, $I_B$-, $I_C$- and $I_D$-states, were observed by pulse proteolysis analysis at 25°C, where the $I_B$- and $I_C$-states are the main forms in the slow unfolding process of this protein. Here, we examined the slow unfolding pathway of Tk-RNase H2 by pulse proteolysis using mutants. For the stabilized variant, D7N, the life time of $I_A$- and $I_B$-states decreased but the $I_C$-state appeared earlier at 25°C, indicating the stabilization of the $I_C$-state. The $I_A$- and $I_B$-states were not observed in the destabilized variant, L33A, at 25°C, whereas in the wild-type these two states disappeared at 50°C. Our results suggest that at higher temperatures the $I_C$-state is the real native state of Tk-RNase H2, whereas the native, $I_A$- and $I_B$-states at 25°C are artificial forms at lower temperatures.

**Keywords:** Ribonuclease H2; *Thermococcus kodakarensis*; Unfolding intermediate; Subtilisin

## Introduction

Ribonuclease H2 from the hyperthermophile, *Thermococcus kodakarensis* (Tk-RNase H2), is a monomer, consists of 228 residues and has a molecular weight of 26 kDa [1]. RNase H hydrolyzes only the RNA strand of an RNA/DNA hybrid [2]. The enzyme is ubiquitously present in various organisms and is involved in DNA replication and repair. RNase H is classified into two major types according to sequence similarity, Type 1 and Type 2 RNase H [3]. Tk-RNase H2 is a Type 2 RNase H. The crystal structures of Tk-RNase H2 and several variants have been determined [4-6]. The stability and folding/unfolding experiments of Tk-RNase H2 are well documented [7-14]. Tk-RNase H2 is highly stable, and its stabilization mechanism is characterized by its remarkably slow unfolding. Hydrophobic and proline mutants of Tk-RNase H2 showed that hydrophobic effects were responsible for the slow unfolding and not proline residues.

In a previous study, we monitored the intermediate structures of Tk-RNase H2 in the slow unfolding pathway using pulse proteolysis and a super-stable protease in the presence of the denaturant guanidine hydrochloride (GdnHCl) [14]. Subtilisin from the hyperthermophilic archaeon *T. kodakarensis* (Tk-subtilisin) is a protease that displays high stability and activity at high temperatures, and is stable in the presence of chemical denaturants [15-25]. We successfully determined regions that constitute the kinetic unfolding intermediates and observed the unfolding behavior of Tk-RNase H2. Tk-RNase H2 includes multiple intermediate forms, $I_A$-, $I_B$-, $I_C$- and $I_D$-states, during the unfolding process [14]. The unfolding reaction of the $I_B$- and $I_C$-states is rate-limiting in the slow unfolding process of Tk-RNase H2. The results also showed that slow unfolding is attributed to the N-terminal region and conformational changes to the C-terminal region occur during unfolding or with an increase in temperature.

In this report, to characterize the unfolding process of Tk-RNase H2 in more detail, we have examined the slow unfolding pathway of Tk-RNase H2 by pulse proteolysis using selected mutants. The mutant D7N is a stabilized variant of the wild-type protein [8], whereas L33A is a destabilized variant [9]. Both mutation sites are located in the N-terminal domain. The pulse proteolysis results of the two mutants differed to that of the wild-type protein. We also confirmed the results using D7N-F20 and L33A-F20, which are derived from residues 1–176 Tk-RNase H2 (F20) [14]. F20 corresponds to the $I_B$-state in the unfolding pathway of Tk-RNase H2. F20 is a digested form in the C-terminal region. Based on the results obtained, we discuss the slow unfolding pathway of Tk-RNase H2.

## Methods

### Plasmids, overproduction and purification of target proteins

Plasmids for the overexpression of Tk-RNase H2, F20, D7N and L33A were constructed as described previously [1,8,9,14]. Plasmids for the overexpression of the mutant D7N-F20 and L33A-F20 were constructed from F20 using standard recombinant DNA techniques. Tk-RNase H2 and its variants were overproduced and purified as described previously [1,8,9,14]. Protein purity was analyzed by SDS-PAGE using a 15% polyacrylamide gel and stained using Coomassie Brilliant Blue staining.

### Kinetic experiments on GdnHCl-induced unfolding

Unfolding reactions were followed by CD measurements at 220 nm, as described previously [14]. The optical path length was 1 cm. The kinetic data were analyzed using:

$$A(t) - A(\infty) = \Sigma A_i e^{-ki\,t} \quad (1)$$

where $A(t)$ is the value of the CD signal at a given time $t$, $A(\infty)$ is the value when no further change is observed, $ki$ is the apparent rate constant of the $i$th kinetic phase and $Ai$ is the amplitude of the $i$th phase. The fitting used SigmaPlot (SYSTAT, IL). All kinetic experiments were

***Corresponding author:** Kazufumi Takano, Department of Biomolecular Chemistry, Kyoto Prefectural University, Kyoto, Japan, Tel: +81-75-703-5654; Fax: +81-75-703-5654; E-mail: takano@kpu.ac.jp

**Received:** August 30, 2015; **Accepted:** October 19, 2015; **Published** October 22, 2015

**Citation:** Shima K, Nagao A, Okada J, Sano S, Takano K (2015) Slow Unfolding Pathway of the Hyperthermophilic Tk-RNase H2 Examined by Pulse Proteolysis Using Mutant Proteins. Biochem Anal Biochem 4: 213. doi:10.4172/2161-1009.1000213

performed in 20 mM Tris-HCl, pH 9.0. The protein concentration was 0.032–0.16 mg $ml^{-1}$.

### Pulse proteolysis in kinetic unfolding by Tk-subtilisin

The protein was unfolded in 20 mM Tris-HCl (pH 9.0) containing 4 M GdnHCl at 25 or 50°C. Reactions were dispensed into aliquots (50 µl). At designated time points, 2 µl Tk-subtilisin at several concentrations in 10 mM acetate buffer (pH 5.0) was added to each aliquot. After 45 s, the reaction was quenched by 10% (w/v) TCA. Proteins were precipitated using 10% (w/v) TCA, washed with 70% acetone and analyzed by 15% tricine-SDS-PAGE [14]. The concentrations of Tk-RNase H2, the variants and Tk-subtilisin were optimized at each experiment depending on the stability and unfolding rate of Tk-RNase H2 and its variants. The amount of protein was estimated from the intensity of the band visualized with Coomassie Brilliant Blue staining using image J [26].

## Results and Discussion

### Stability of Tk-RNase H2 and its variants

The thermal unfolding properties of Tk-RNase H2, D7N, L33A and F20 have been examined previously [8,9,14]. The changes in the $T_m$ value ($\Delta T_m$) of the variants compared with the wild-type Tk-RNase H2 are summarized in Table 1. D7N is stabilized, whereas L33A is destabilized. The $T_m$ value of F20 is slightly higher than the $T_m$ value of the wild-type protein.

### Unfolding of Tk-RNase H2 and its variants examined by CD spectroscopy

The kinetics of GdnHCl-induced unfolding of Tk-RNase H2 and its variants were examined at 25 or 50°C. The reaction was initiated by a jump to 3.2 or 4 M GdnHCl followed by far-UV CD signal recording at 220 nm. The kinetic unfolding curves are shown in Figure 1. RNase H2 and the D7N mutant unfolding at 25°C (Figure 1A and 1B) was characterized by signal changes in the far-UV CD within dead times (~2 s). This indicates a burst phase in the kinetics of the slow unfolding of Tk-RNase H2 and D7N. The burst phase, which was ~30% of the total signal changes between the unfolded and native states, was followed by a slower observable phase. The slow unfolding phase after the burst phase was approximated as a first-order reaction. In the other experiments at 25°C (Figure 1C and Figure 1E-1G), the burst phase signal was not detected in the kinetic curves. The burst phase of Tk-RNase H2 at 50°C was about 20% of the total signal changes between the unfolded and native states, indicating a decrease in the burst phase with an increase in temperature (Figure 1D) [14]. The kinetic trace was approximated to a first-order reaction. The unfolding rate constants are listed in Table 2.

The unfolding rates of D7N and L33A are slower and faster, respectively, than the unfolding rate of the wild-type protein, and clearly dependent on their stability. This pattern was also observed for F20 and its variants. The unfolding rate constant of F20 was equal to Tk-RNase H2 at 25 and 50°C. The results indicate that F20 is a rate-limiting factor in the slow unfolding process of Tk-RNase H2.

| | $\Delta T_m$ (°C) |
|---|---|
| Tk-RNase H2 (wild-type) | (85.7)[a] |
| D7N | 3.1[b] |
| L33A | –11.9[c] |
| F20 | 1.1[d] |

[a]$T_m$ value. Data from ref. [14].

[b]Data from ref. [8].

[c]Data from ref. [9].

[d]Data from ref. [14].

**Table 1:** Change in the $T_m$ value ($\Delta T_m$) of the variants compared with Tk-RNase H2 at pH 9.0.

### Unfolding of Tk-RNase H2 and its variants examined by pulse proteolysis

Pulse proteolysis experiments were performed after the protein was unfolded in 20 mM Tris-HCl (pH 9.0) containing 4 M GdnHCl. The remaining intact protein and its degradation products were detected by tricine-SDS-PAGE (sodium dodecyl sulfate polyacrylamide gel electrophoresis), as shown in Figure 2.

In Figure 2A, an intact band and several cleavage products of Tk-RNase H2 were observed [14]. The intact band decreased in intensity to less than half the initial value in 0.5 min. The amount of the intact protein at 0.5 and 1 min was less than that at 2 to 16 min. These results indicate that a proportion of intact protein was digested ($I_A$-state) in the early stages of unfolding. Two heavy chain fragments (fragments 22 and 20) at ~20 kDa appeared. The fragments correspond to the $I_B$-state. After 2 min, the amount of intact protein increased, which represents the $I_C$-state. The bands of fragments 20 and 22 decreased in intensity at 30 to 60 min, but the intensity of the band representing the intact protein was unaffected. That is, the $I_A$-state changes to forms ($I_B$- and $I_C$-states) that are partially and fully, respectively, resistant to Tk-subtilisin, and the $I_B$-state moves to the $I_C$-state during unfolding in GdnHCl. The Tk-subtilisin resistant form ($I_C$-state) of Tk-RNase H2 gradually unfolded via the $I_D$-state and was subsequently degraded by Tk-subtilisin.

The result of pulse proteolysis at 25°C of D7N unfolding (Figure 2B) was similar to the wild-type unfolding result (Figure 2A). However, the $I_A$- and $I_B$-states decreased and the $I_C$-state appeared earlier, indicating the stabilization of the $I_C$-state by the D7N mutation. For L33A, Figure 2C shows that the intact band decreased over time, but few degradation products were detected. This indicates the disappearance of the $I_A$- and $I_B$-states in L33A unfolding. A similar result was also observed in the wild-type unfolding at 50°C (Figure 2D). L33A was degraded faster than the wild-type protein at 50°C, depending on their unfolding rates (Table 2). These results suggest that the unfolding of the destabilized variant, L33A, at 25°C and the wild-type protein at 50°C starts from the $I_C$-state. This is related to the disappearance and decrease of the burst phase signal during the kinetic unfolding of L33A at 25°C and the wild-type protein at 50°C, respectively (Figure 1C and 1D).

F20 loses the C-terminal region of Tk-RNase H2. The proteolysis experiments of F20 at 25°C indicated that the band intensities of the intact protein gradually disappeared over time and other bands did not appear (Figure 2E). The result is similar to that observed for D7N-F20 and L33A-F20 (Figure 2F and Figure 2G), whereas the degradation rate of D7N-F20 and L33A-F20 was slower and faster, respectively, than that seen for F20, and is dependent on the unfolding rate of the protein (Table 2). The results suggest that the mutations affect the stability of the $I_B$-state.

### Energy diagram of the unfolding pathway of Tk-RNAse H2

Figure 3A shows the schematic illustration for the energy diagram of the unfolding pathway of Tk-RNase H2 at 25°C and is based on previous work [14]. The N state changes to the $I_B$- and $I_C$-states, which are stable intermediate forms, through the $I_A$-state. The intermediate forms unfold via the $I_D$-state. In D7A and L33A, the mutations stabilize

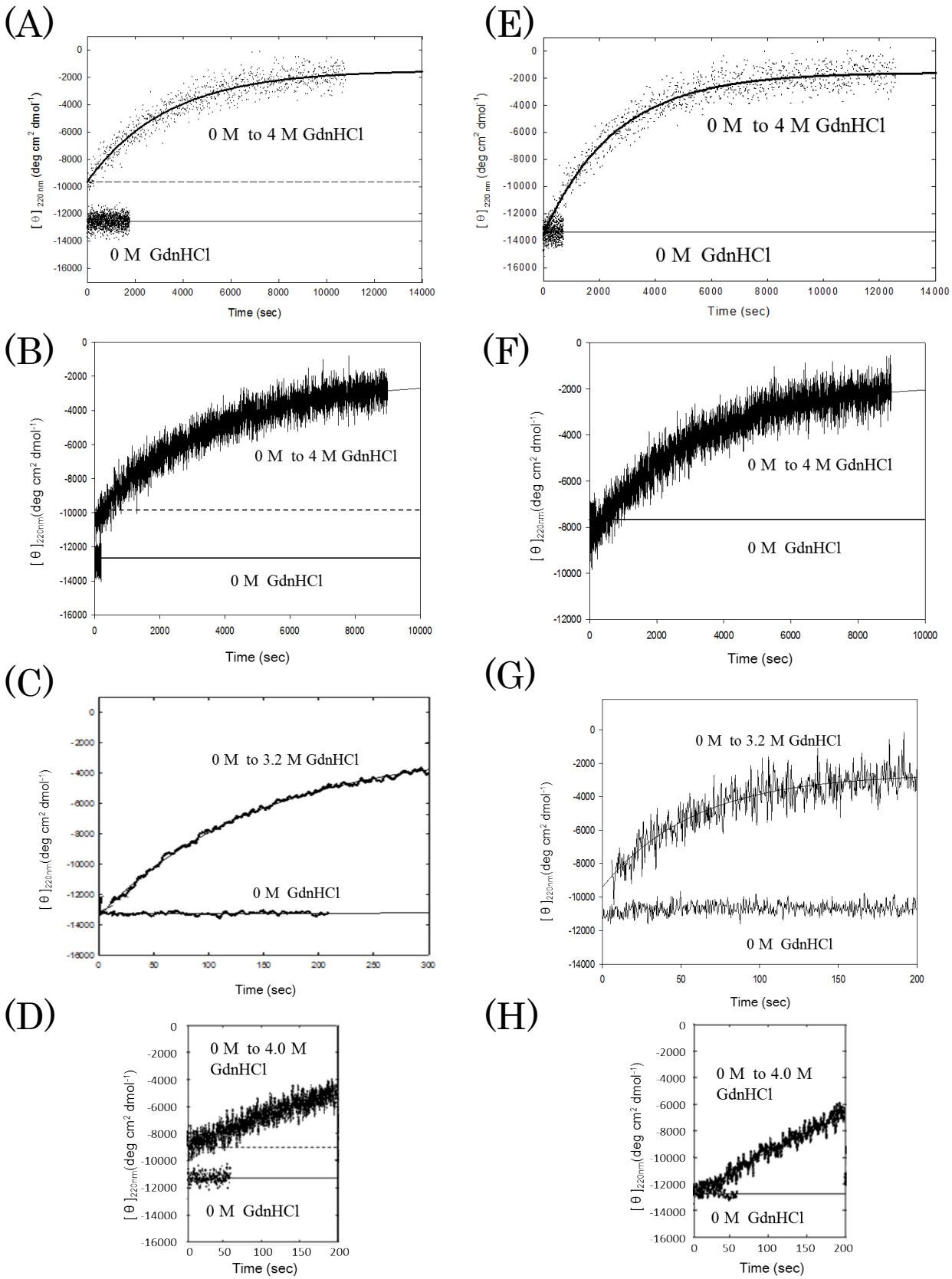


**Figure 1:** Kinetic unfolding curves of Tk-RNase H2 and its variants. Unfolding was initiated by rapid dilution of the protein from native to unfolding conditions (0 M to 3.2 M or 4 M GdnHCl), and monitored by CD at 220 nm. (A) Tk-RNase H2 at 25°C. (B) D7N at 25°C. (C) L33A at 25°C. (D) Tk-RNase H2 at 50°C. (E) F20 at 25°C. (F) D7N-F20 at 25°C. (G) L33A-F20 at 25°C. (H) F20 at 50°C. The native state (0 M GdnHCl) was monitored by CD at 220 nm.

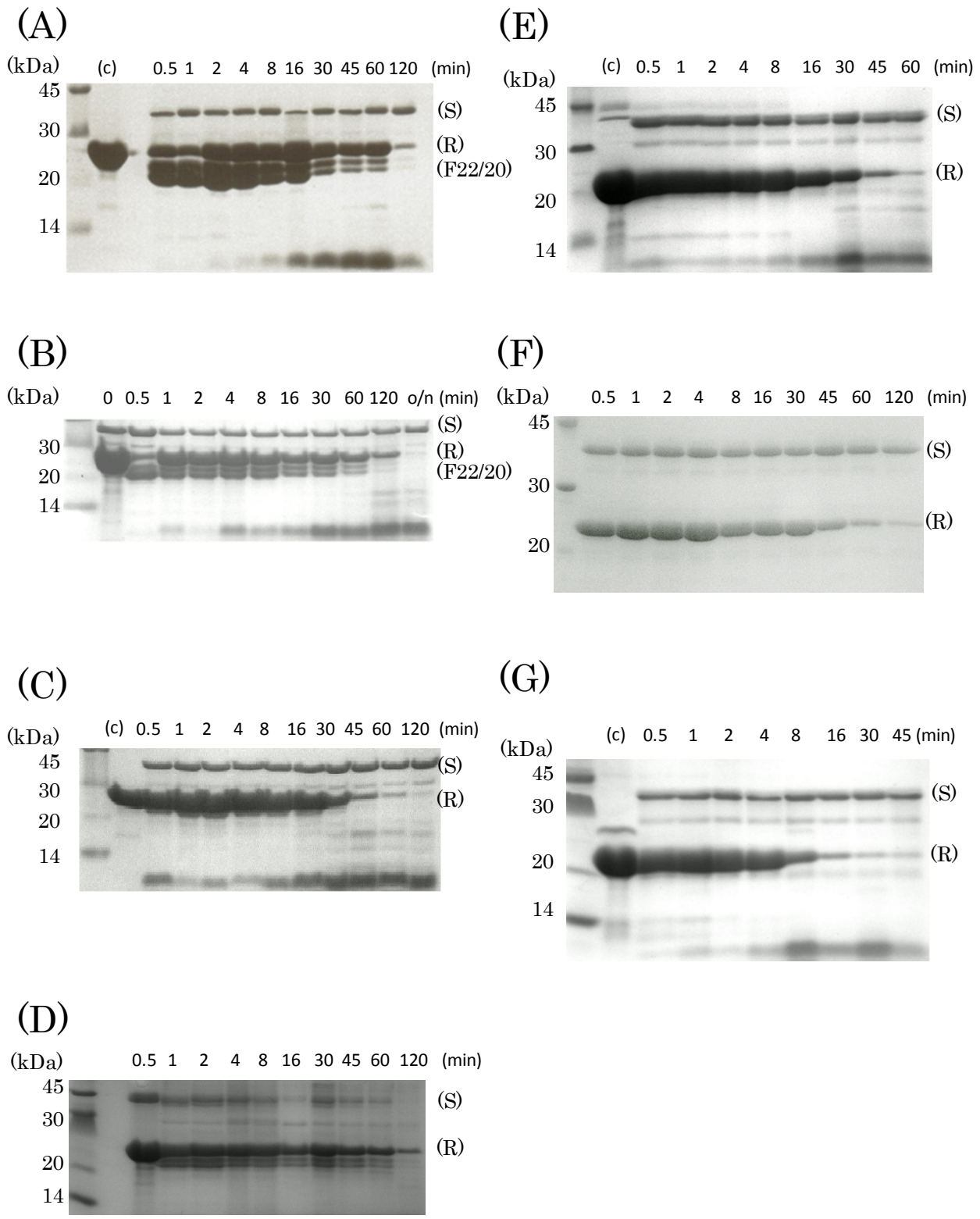


**Figure 2:** Pulse proteolysis in kinetic unfolding of Tk-RNase H2 and its variants by Tk-subtilisin. The protein was unfolded by adding 4 M GdnHCl. At each time point (0.5-120 min), the sample was dispensed into tubes, and proteolysis was performed by the addition of Tk-subtilisin and the sample incubated for 45 s. Proteolysis was quenched by 10% TCA and the products were quantified by tricine-SDS-PAGE. Lanes (c) contained only Tk-RNase H2 or each mutant. (A) Tk-RNase H2 at 25°C. (B) D7N at 25°C. (C) L33A at 25°C. (D) Tk-RNase H2 at 50°C. (E) F20 at 25°C. (F) D7N-F20 at 25°C. (G) L33A-F20 at 25°C. Bands corresponding to Tk-subtilisin (S), Tk-RNase H2 and its variants (R) and cleavage products (F22/20) are indicated

| | 25°C | 50°C |
|---|---|---|
| Tk-RNase H2 (wild-type) | [4M GdnHCl] $4.2 \times 10^{-4} \pm 0.5 \times 10^{-4}$[a] | [4M GdnHCl] $4.2 \times 10^{-3} \pm 0.8 \times 10^{-3}$[a] |
| D7N | [4M GdnHCl] $2.9 \times 10^{-4} \pm 0.5 \times 10^{-4}$ | – |
| L33A | [3.2M GdnHCl] $1.3 \times 10^{-2} \pm 0.6 \times 10^{-2}$ | – |
| F20 | [4M GdnHCl] $6.4 \times 10^{-4} \pm 0.5 \times 10^{-4}$[a] | [4M GdnHCl] $3.7 \times 10^{-3} \pm 0.8 \times 10^{-3}$[a] |
| D7N-F20 | [4M GdnHCl] $3.2 \times 10^{-4} \pm 0.5 \times 10^{-4}$ | – |
| L33A-F20 | [3.2M GdnHCl] $1.4 \times 10^{-2} \pm 0.6 \times 10^{-2}$ | – |

[a]Data from ref. [14].

**Table 2:** Unfolding Rate Constants ($s^{-1}$) of Tk-RNase H2 and Its Variants in GdnHCl at pH 9.0.

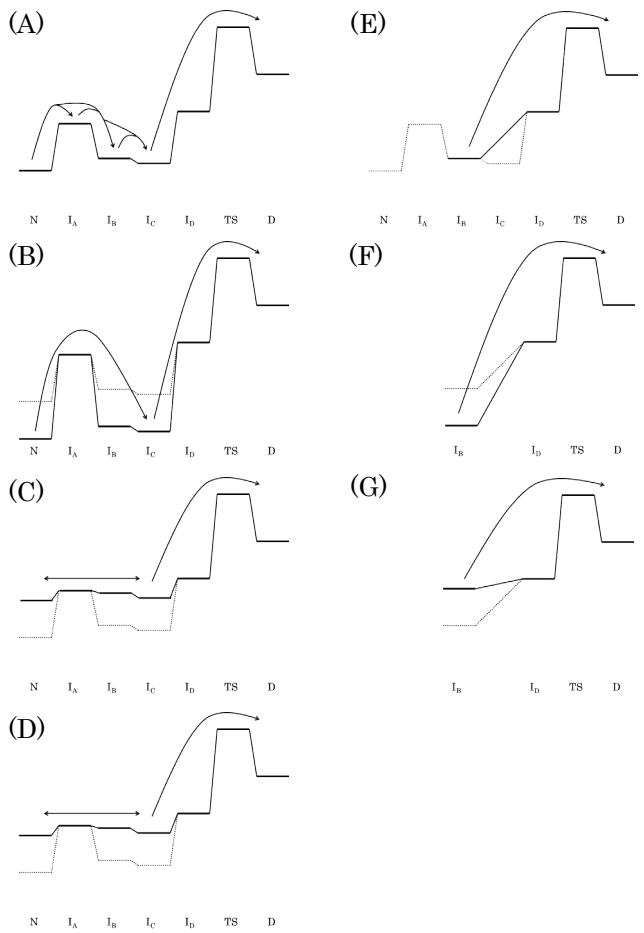


**Figure 3:** Schematic illustrations for the energy diagram of the unfolding process of Tk-RNase H2 and its variants. (A) Tk-RNase H2 at 25°C. (B) D7N at 25°C. (C) L33A at 25°C. (D) Tk-RNase H2 at 50°C. (E) F20 at 25°C. (F) D7N-F20 at 25°C. (G) L33A-F20 at 25°C. TS, transition state. Arrows indicate the main unfolding routes. Dotted lines in B-E and F-G are the energy diagrams of Tk-RNase H2 and F20 at 25°C, respectively.

and destabilize, respectively, the N-terminal domain, because both mutation sites are located at the N-terminal domain. The N-terminal domain contributes to the stabilization of the N-, $I_B$- and $I_C$-states [14]. This means that the N-, $I_B$- and $I_C$-states of D7N are more stable than those of Tk-RNase H2, but the stability of the $I_A$-state is comparable with that of the wild-type (Figure 3B). Since the $I_A$-state is less stable than the N-, $I_B$- and $I_C$-states of D7N, the $I_A$-state was detected only during the burst phase signal in the kinetic unfolding curve of the CD measurements (Figure 1B), but not by pulse proteolysis (Figure 2B). Furthermore, the change from $I_B$-state to $I_C$-state in D7N was faster than that in the wild-type (Figure 2A and 2B), resulted from the larger difference in stability between the $I_A$-state and N-/$I_B$/$I_C$-states of D7N than that of the wild-type protein (Figure 3A and 3B). For L33A, the N-, $I_B$- and $I_C$-states are destabilized, so that the energy levels of the N-, $I_A$-, $I_B$- and $I_C$-states are the same degree (Figure 3C). In the native environment at 25°C, L33A fluctuates among these states. Consequently, L33A apparently unfolds from the $I_C$-state. Likewise, the unfolding of Tk-RNase H2 at 50°C starts from the $I_C$-state (Figure 3D). Of course, it is difficult to judge the start form, N-state or $I_C$-state, from the result of pulse proteolysis. The other results, such as pulse proteolysis of the other mutants and kinetic unfolding experiments, however, support this idea. The $I_B$-states of D7N-F20 and L33A-F20 are stable and unstable, respectively, compared with the stability of this state of F20 (Figure 3E-3G). The unfolding rates of D7N-F20 and L33A-F20 are slower and faster than that of F20, respectively. This information suggests that the $I_C$-state is the native state of Tk-RNase H2 at high temperatures in nature.

## Conformations of the C-terminal region

From the N-state to $I_C$-state, the C-terminal region changes conformation. The structural and mutational analysis of Tk-RNase H2 showed that the C-terminal region plays an important role in substrate binding and changes conformation during this process [4]. Therefore, the C-terminal region of Tk-RNase H2 can readily change its conformation. The "native form" of the C-terminal region of Tk-RNase H2 at high temperatures would shift to a more stable artificial state at lower temperatures. Such non-natural states of thermophilic proteins at lower temperatures have been reported [27-29]. Recombinant catalase I from *Bacillus stearothermophilus* and glutamate dehydrogenases from *Pyrobaculum islandicum* and *T. kodakarensis* expressed at moderate temperatures convert into active forms following heat treatment. For Tk-RNase H2, the N-state is the most stable form at lower temperatures and the $I_C$-state is the active form at higher temperatures, where the host organism, *T. kodakarensis*, can grow.

## Conclusion

Tk-RNase H2 unfolds through the multiple intermediate states at moderate temperatures. Our pulse proteolysis analysis of the wild-type and mutant proteins at different temperatures reveals that the unfolding pathway at higher temperatures is more simply than that at lower temperatures. We could observe the artificial forms at lower temperatures and the real native state at higher temperatures.

### Acknowledgments

This work was supported in part by Grants (22710215 and 25440194) from the Ministry of Education, Culture, Sports, Science and Technology of Japan.

### References

1. Haruki M, Hayashi K, Kochi T, Muroya A, Koga Y, et al. (1998) Gene cloning and characterization of recombinant RNase HII from a hyperthermophilic archaeon. J Bacteriol 180: 6207-6214.
2. Crouch RJ, Dirksen ML (1982) Ribonuclease H: In Nuclease. Linn SM, Roberts RJ, Cold Spring Harbor Laboratory: Cold Spring Harbor, NY.
3. Ohtani N, Haruki M, Morikawa M, Kanaya S (1999) Molecular diversities of RNases H. J Biosci Bioeng 88: 12-19.
4. Muroya A, Tsuchiya D, Ishikawa M, Haruki M, Morikawa M, et al. (2001) Catalytic center of an archaeal type ribonuclease H as revealed by X-ray crystallographic and mutational analyses. Protein Sci 10: 707-714.

5. Takano K, Endo S, Mukaiyama A, Chon H, Matsumura H, et al. (2006) Structure of amyloid beta fragments in aqueous environments. FEBS J 273: 150-158.

6. Takano K, Katagiri Y, Mukaiyama A, Chon H, Matsumura H, et al. (2007) Conformational contagion in a protein: structural properties of a chameleon sequence. Proteins 68: 617-625.

7. Mukaiyama A, Takano K, Haruki M, Morikawa M, Kanaya S (2004) Kinetically robust monomeric protein from a hyperthermophile. Biochemistry 43: 13859-13866.

8. Mukaiyama A, Haruki M, Ota M, Koga Y, Takano K, et al. (2006) A hyperthermophilic protein acquires function at the cost of stability. Biochemistry 45: 12673-12679.

9. Dong H, Mukaiyama A, Tadokoro T, Koga Y, Takano K, et al. (2008) Hydrophobic effect on the stability and folding of a hyperthermophilic protein. J Mol Biol 378: 264-272.

10. Mukaiyama A, Koga Y, Takano K, Kanaya S (2008) Osmolyte effect on the stability and folding of a hyperthermophilic protein. Proteins 71: 110-118.

11. Takano K, Higashi R, Okada J, Mukaiyama A, Tadokoro T, et al. (2009) Proline effect on the thermostability and slow unfolding of a hyperthermophilic protein. J Biochem 145: 79-85.

12. Mukaiyama A, Takano K (2009) Slow unfolding of monomeric proteins from hyperthermophiles with reversible unfolding. Int J Mol Sci 10: 1369-1385.

13. Okada J, Okamoto T, Mukaiyama A, Tadokoro T, You DJ, et al. (2010) Evolution and thermodynamics of the slow unfolding of hyperstable monomeric proteins. BMC Evol Biol 10: 207.

14. Okada J, Koga Y, Takano K, Kanaya S (2012) Slow unfolding pathway of hyperthermophilic Tk-RNase Hexamined by pulse proteolysis using the stable protease Tk-subtilisin. Biochemistry 51: 9178-9191.

15. Pulido M, Saito K, Tanaka S, Koga Y, Morikawa M, et al. (2006) Ca2+-dependent maturation of subtilisin from a hyperthermophilic archaeon, Thermococcus kodakaraensis: the propeptide is a potent inhibitor of the mature domain but is not required for its folding. Appl Environ Microbiol 72: 4154-4162.

16. Tanaka S, Saito K, Chon H, Matsumura H, Koga Y, et al. (2007) Crystal structure of unautoprocessed precursor of subtilisin from a hyperthermophilic archaeon. J Biol Chem 282: 8246-8255.

17. Tanaka S, Matsumura H, Koga Y, Takano K, Kanaya S (2007) Four new crystal structures of Tk-subtilisin in unautoprocessed, autoprocessed and mature forms: Insight into structural changes during maturation. J Mol Biol 372: 1055-1069.

18. Pulido MA, Koga Y, Takano K, Kanaya S (2007) Directed evolution of Tk-subtilisin from a hyperthermophilic archaeon: identification of a single amino acid substitution responsible for low-temperature adaptation. Protein Eng Des Sel 20: 143-153.

19. Pulido MA, Tanaka S, Sringiew C, You DJ, Matsumura H, et al. (2007) Requirement of left-handed glycine residue for high stability of the Tk-subtilisin propeptide as revealed by mutational and crystallographic analyses. J Mol Biol 374: 1359-1373.

20. Tanaka S, Takeuchi Y, Matsumura H, Koga Y, Takano K, et al. (2008) Crystal structure of Tk-subtilisin folded without propeptide: requirement of propeptide for acceleration of folding. FEBS Lett 582: 3875-3878.

21. Tanaka S, Matsumura H, Koga Y, Takano K, Kanaya S (2009) Identification of the interactions critical for propeptide-catalyzed folding of Tk-Subtilisin. J Mol Biol 394: 306-319.

22. Takeuchi Y, Tanaka S, Matsumura H, Koga Y, Takano K, et al. (2009) Requirement of a unique Ca(2+)-binding loop for folding of Tk-subtilisin from a hyperthermophilic archaeon. Biochemistry 48: 10637-10643.

23. Uehara R, Takeuchi Y, Tanaka S, Takano K, Koga Y, et al. (2012) Requirement of Ca(2+) ions for the hyperthermostability of Tk-subtilisin from Thermococcus kodakarensis. Biochemistry 51: 5369-5378.

24. Koga Y, Tanaka S, Sakudo A, Tobiume M, Aranishi M, et al. (2014) Proteolysis of abnormal prion protein with a thermostable protease from Thermococcus kodakarensis KOD1. Appl Microbiol Biotechnol 98: 2113-2120.

25. Hirata A, Sakudo A, Takano K, Kanaya S, Koga Y (2015) Effects of surfactant and a hyperthermostable protease on infectivity of scrapie-infected mouse brain homogenate. J Biotechnol Biomater 5: 194.

26. Schneider CA, Rasband WS, Eliceiri KW (2012) NIH Image to Image J: 25 years of image analysis. Nat Methods 9: 671-675.

27. Kobayashi C, Suga Y, Yamamoto K, Yomo T, Ogasahara K, et al. (1997) Thermal conversion from low- to high-activity forms of catalase I from Bacillus stearothermophilus. J Biol Chem 272: 23011-23016.

28. Goda S, Kojima M, Nishikawa Y, Kujo C, Kawakami R, et al. (2005) Intersubunit interaction induced by subunit rearrangement is essential for the catalytic activity of the hyperthermophilic glutamate dehydrogenase from Pyrobaculum islandicum. Biochemistry 44: 15304-15313.

29. Izumikawa N, Shiraki K, Nishikori S, Fujiwara S, Imanaka T, et al. (2004) Biophysical analysis of heat-induced structural maturation of glutamate dehydrogenase from a hyperthermophilic archaeon. J Biosci Bioeng 97: 305-309.